International Journal of Solids and Structures 151 (2018) 135–144

Contents lists available at ScienceDirect

International Journal of Solids and Structures

journal homepage: www.elsevier.com/locate/ijsolstr

Study on the effect of tension-compression asymmetry on the cylindrical cup forming of an AA2090-T3 alloy

P.D. Barros[a,*], J.L. Alves[b], M.C. Oliveira[a], L.F. Menezes[a]

[a] CEMMPRE, Department of Mechanical Engineering, University of Coimbra, Polo II, Rua Luís Reis Santos, Pinhal de Marrocos, 3030-788 Coimbra, Portugal
[b] CMEMS, Center for Microelectromechanical Systems Research Unit, University of Minho, Campus de Azurém, 4800-058 Guimarães, Portugal

ARTICLE INFO

Article history:
Revised 1 May 2017
Available online 28 June 2017

Keywords:
Sheet metal forming
Finite element method
CPB06 yield criterion
Tension-compression asymmetry
Anisotropy parameters identification

ABSTRACT

In this work, the Cazacu et al. (2006) is adopted to study the effect of the asymmetry between the tensile and the compressive plastic behavior in sheet metal forming. The example selected for this analysis is a cylindrical cup drawing, since it involves tensile and compressive stress states (Yoon et al., 2000). The material selected is the 2090-T3 aluminum alloy, since the experimental data available includes both tension and compression yield stress in-plane distributions (Barlat et al., 1991b), which allows the use of a classical strategy for the anisotropy parameters identification. Different sets of parameters are identified for the CPB06, taking or not into account the strength differential (SD) effect and, consequently, considering different sets of experimental data. All numerical simulations are performed with the DD3IMP fully implicit in-house code.

The results show that the earing profile is mainly dictated by the compression *r*-values in-plane directionalities, which are commonly unavailable for thin metallic sheets. The adoption of the CPB06 taking into account the tension-compression asymmetry, with an associated flow rule, enables the simultaneous prediction of both compression yield stress and *r*-values directionalities. The compression yield stresses directionalities seem to play a major role in the thickness prediction. Therefore, it is recommended the use of a yield criterion that is flexible enough to describe both the yield stresses and *r*-values directionalities, including the ones in compression, even for materials that present a small SD effect.

1. Introduction

Sheet metal forming processes are nowadays designed and optimized virtually using finite element analysis (FEA). Such virtual try-out approach is consensually accepted as the main reason for the huge decrease in the time-to-market life cycle and for the notable savings in terms of money, time and effort in the design, production and process set-up of new formed parts. The deep drawing process, which consists in giving to a thin metal sheet, initially flat, the desired shape, allows high volume production of sheet metal parts of different complexities. Thus, one of the most important industries exploring the advantages of this kind of process is the automotive, due to the high production rates. However, the success of finite elements solvers on the design and optimization of sheet metal formed parts is strongly dependent on their ability to accurately describe the material's mechanical behavior.

Sheet metals, due to their crystallographic structure and the way they are obtained, generally exhibit anisotropy of their mechanical properties. In fact, the rolling process induces a particular type of anisotropic behavior, characterized by the symmetry of the mechanical properties with respect to the three orthogonal planes, i.e. orthotropy (Banabic, 2010). As this process makes the metal sheets orthotropic, different mechanical behaviors are expected for different loading directions and conditions. Moreover, sheet metal forming processes are carried out with inhomogeneous deformation and under multiaxial strain paths.

Phenomenological models are the most widely used to describe the elastoplastic response of metallic sheets, since they are computationally efficient when compared with microscopic based models. Also, it is common to adopt an associated flow rule, meaning that the material's orthotropic behavior is modeled by a yield surface, which describes the yielding and the plastic flow of the material. This dual role of the yield surface requires a particular care and accuracy in its modeling and numerical implementation.

For isotropic materials, the Tresca (1864) and von Mises (1913) are the most widely used yield criteria. As for yield criteria for materials with orthotropic behavior, the Hill (1948) quadratic function was the first proposed for anisotropic materials and it is still the most widely used. Nevertheless, other formulations have

* Corresponding author.
E-mail address: pedro.barros@dem.uc.pt (P.D. Barros).

http://dx.doi.org/10.1016/j.ijsolstr.2017.06.034
0020-7683/

been proposed to improve the description of the mechanical behavior of orthotropic metallic materials, in particular aluminum and its alloys (e.g. Barlat et al., (2005, 2003, 1997b, 1991a), Banabic et al., (2000), Cazacu and Barlat (2003, 2001), Comsa and Banabic, (2007) Yoshida et al., (2013)). In fact, several authors refer that an improved modeling of both the materials yield stresses and *r*-values in-plane directionalities improves the accuracy of the earing profile prediction on the deep drawing of cylindrical cups (Barros et al., 2016a, 2015a; Chung et al., 2011; Mulder and Vegter, 2011; Yoon et al., 2011).

In most numerical analysis of metal forming processes, the yield surface is assumed to possess a point-symmetry with respect to its center, such that a stress state and its reverse state have the same absolute value (Banabic, 2010). However, it has been shown that this can be an unrealistic approximation, even for cubic metals (both face centered cubic (FCC) and body centered cubic (BCC)) (Barlat et al., 1991b). Therefore, Cazacu and Barlat (2004) extended the Drucker (1949) isotropic yield function to the anisotropic case through invariants generalizing, to enable the description of both the materials anisotropy and the tension-compression asymmetry, also known as strength differential effect. Later, Cazacu et al. (2006) presented another yield criterion that enables describing also both effects using a linear transformation, with a fourth-order tensor, of the deviatoric stress tensor. This formulation has the advantage of enabling the adoption of several linear transformations in order to more accurately capture the material's anisotropic behavior (Plunkett et al., 2006; Tritschler et al., 2014). However, the adoption of several linear transformations means that the yield surface modeling becomes more complex due to the higher number of material anisotropy parameters involved, also requiring more experimental data to enable its identification.

The material anisotropy parameters identification must be performed such that a given yield criterion reproduces the materials mechanical behavior as close as possible. This procedure is typically based in an optimization problem regarding the minimization of an error function, which evaluates the difference between the estimated values and the experimental ones. The key idea is to identify the material parameters in order to numerically obtain the same results as the experimental ones.

In this work, the DD3IMP in-house code (Menezes and Teodosiu, 2000; Neto et al., 2015; Oliveira et al., 2008) is used to perform the numerical simulation of a circular cup drawing, which was chosen since it involves tensile and compressive stress states (Yoon et al., 2000). The numerical simulations are performed with two yield criteria: (i) the CPB06 yield criterion, which accounts for both tension-compression asymmetry and orthotropic plastic behavior; and (ii) the Cazacu and Barlat (2001) yield criterion, which is known for its flexibility in describing highly anisotropy in-plane behavior, due to the high number of anisotropy parameters, but it does not allows the description of the SD effect. These yield criteria are described in the following section. The identification strategy is discussed in section three, assuming that only one linear transformation of the deviatoric stress tensor is applied in the CPB06 yield criterion and the homogeneity parameter $a=2$. In section four, the numerical model adopted for the cup drawing is presented and the anisotropy parameters identification procedures are applied for a 2090-T3 aluminum alloy. For the CPB06, different sets of parameters are identified, taking or not into account the SD effect and, consequently, using different sets of experimental data. The results obtained for the punch force evolution, the earing profile and the thickness distribution are discussed. For the earing profile, the numerical results are also compared with the ones obtained with an analytical function (Yoon et al., 2011), trying to separate the effect of the compression yield stress and *r*-value directionalities. Finally, in section five, the main conclusions are summarized.

2. Anisotropic yield criteria

The Cazacu et al. (2006) yield criterion (CPB06) is adopted in this work since it allows the description of both the orthotropic behavior and the SD effect, i.e. tension-compression asymmetry. The equivalent stress $\bar{\sigma}$ associated with the orthotropic form of the CPB06 yield criterion is defined as

$$\bar{\sigma} = B\left[(|s_1| - k\,s_1)^a + (|s_2| - k\,s_2)^a + (|s_3| - k\,s_3)^a\right]^{\frac{1}{a}}, \tag{1}$$

where the exponent a, considered to be a positive integer, and k are material parameters and s_1, s_2 and s_3 are the principal values of the tensor $\mathbf{s}$. This tensor is determined following the linear transformation proposed by Barlat et al. (1997b), such that $\mathbf{s}=\mathbf{C}:\boldsymbol{\sigma}'$, where $\boldsymbol{\sigma}'$ is the deviatoric stress tensor and $\mathbf{C}$ is the constant 4th-order transformation tensor. Using the Voigt notation, such as

$$\begin{Bmatrix}\sigma'_{11}\\ \sigma'_{22}\\ \sigma'_{33}\\ \sigma'_{23}\\ \sigma'_{13}\\ \sigma'_{12}\end{Bmatrix} = \begin{Bmatrix}\sigma'_{1}\\ \sigma'_{2}\\ \sigma'_{3}\\ \sigma'_{4}\\ \sigma'_{5}\\ \sigma'_{6}\end{Bmatrix}, \tag{2}$$

the tensor $\mathbf{C}$, which for 3-D stress conditions involves 9 independent anisotropy coefficients, is expressed in the principal axis of anisotropy as

$$\mathbf{C} = \begin{bmatrix} C_{11} & C_{12} & C_{13} & 0 & 0 & 0\\ C_{12} & C_{22} & C_{23} & 0 & 0 & 0\\ C_{13} & C_{23} & C_{33} & 0 & 0 & 0\\ 0 & 0 & 0 & C_{44} & 0 & 0\\ 0 & 0 & 0 & 0 & C_{55} & 0\\ 0 & 0 & 0 & 0 & 0 & C_{66}\end{bmatrix}. \tag{3}$$

B is a constant defined such that $\bar{\sigma}$ reduces to the tensile yield stress in the rolling direction and is given by

$$B = \left[\frac{1}{(|\phi_1| - k\,\phi_1)^a + (|\phi_2| - k\,\phi_2)^a + (|\phi_3| - k\,\phi_3)^a}\right]^{\frac{1}{a}}, \tag{4}$$

with

$$\begin{Bmatrix}\phi_1\\ \phi_2\\ \phi_3\end{Bmatrix} = \begin{Bmatrix}(2/3)C_{11} - (1/3)C_{12} - (1/3)C_{13}\\ (2/3)C_{21} - (1/3)C_{22} - (1/3)C_{23}\\ (2/3)C_{31} - (1/3)C_{32} - (1/3)C_{33}\end{Bmatrix}. \tag{5}$$

The convexity is guaranteed for any integer $a \geq 2$ and $k \in [-1, 1]$ (Cazacu et al., 2006).

The equivalent stress $\bar{\sigma}$ associated with the isotropic form of the CPB06 yield criterion is defined as in Eq. (1) and, in this case, the constant 4th-order transformation tensor becomes the 4th-order identity tensor, such as $\mathbf{C}=\mathbf{I}$. Considering these conditions and $a=2$, Eq. (4) becomes

$$B = \sqrt{\frac{9/2}{3k^2 - 2k + 3}}. \tag{6}$$

Therefore, if $a=2$ and $k=0$, then $B=\sqrt{3/2}$ and $\bar{\sigma}$ becomes the von Mises equivalent stress. Moreover, for a material presenting isotropic behavior, the coefficient k alone allows for the description of the SD effect, giving a direct measure of the ratio between tensile (σ^{T}) and compressive (σ^{C}) yield stresses (Cazacu et al., 2006). However, for a material presenting orthotropic behavior it is not possible to define a single $\sigma^{\mathrm{T}}/\sigma^{\mathrm{C}}$ ratio. In case of metal sheets, the three principal axis correspond to the rolling direction (RD), the transverse direction (TD) and the normal to the sheet plane direction (ND). Therefore, it is possible to define a ratio between tensile and compressive yield stresses for each axis, which will be labeled $\sigma^{\mathrm{T}}_{\mathrm{RD}}/\sigma^{\mathrm{C}}_{\mathrm{RD}}$, $\sigma^{\mathrm{T}}_{\mathrm{TD}}/\sigma^{\mathrm{C}}_{\mathrm{TD}}$ and $\sigma^{\mathrm{T}}_{\mathrm{ND}}/\sigma^{\mathrm{C}}_{\mathrm{ND}}$, respectively. In this case, the stress ratios depend on both the anisotropy parameters and the k value.

The Cazacu and Barlat (2001) yield criterion (CB2001) is a generalization of the Drucker's isotropic criterion to orthotropy and, in its general form, is given by

$$\bar{\sigma} = \left\{ 27\left[\left(J_2^0\right)^3 - c\left(J_3^0\right)^2 \right] \right\}^{\frac{1}{6}}, \tag{7}$$

where J_2^0 and J_3^0 are the second and third generalized invariants of the deviatoric stress tensor $\boldsymbol{\sigma}'$, defined as

$$\begin{aligned} J_2^0 = {} & \frac{a_1}{6}(\sigma'_{11}-\sigma'_{22})^2 + \frac{a_2}{6}(\sigma'_{11}-\sigma'_{33})^2 \\ & + \frac{a_3}{6}(\sigma'_{11}-\sigma'_{33})^2 + a_4\sigma'^2_{12} + a_5\sigma'^2_{13} + a_6\sigma'^2_{23}, \end{aligned} \tag{8}$$

$$\begin{aligned} J_3^0 = {} & (1/27)(b_1+b_2)\sigma'^3_{11} + (1/27)(b_3+b_4)\sigma'^3_{22} \\ & + (1/27)[2(b_1+b_4)-b_2-b_3]\sigma'^3_{33} \\ & - (1/9)\left(b_1\sigma'_{22}+b_2\sigma'_{33}\right)\sigma'^2_{11} - (1/9)\left(b_3\sigma'_{33}+b_4\sigma'_{11}\right)\sigma'^2_{22} \\ & - (1/9)\left[(b_1-b_2+b_4)\sigma'_{11} + (b_1-b_3+b_4)\sigma'_{22}\right]\sigma'^2_{33} \\ & + (2/9)(b_1+b_4)\sigma'_{11}\sigma'_{22}\sigma'_{33} \\ & - \left(\sigma'^2_{13}/3\right)\left[2b_9\sigma'_{22} - b_8\sigma'_{33} - (2b_9-b_8)\sigma'_{11}\right] \\ & - \left(\sigma'^2_{12}/3\right)\left[2b_{10}\sigma'_{33} - b_5\sigma'_{22} - (2b_{10}-b_5)\sigma'_{11}\right] \\ & - \left(\sigma'^2_{23}/3\right)\left[(b_6-b_7)\sigma'_{11} - b_6\sigma'_{22} - b_7\sigma'_{33}\right] \\ & + 2b_{11}\sigma'_{12}\sigma'_{23}\sigma'_{13}, \end{aligned} \tag{9}$$

where c, a_1,..., a_6 and b_1,..., b_{11} are the anisotropy parameters. σ'_{ij}, $i, j = 1, 2, 3$ are the deviatoric stress tensor components defined in the material frame. The conditions that guarantee the convexity of CB2001 are unknown, except when assuming in-plane isotropic behavior, for which $c \in [-3.75, 2.25]$ (Cazacu and Barlat, 2001). For further details concerning the constitutive model and the its implementation, please refer to (Barros et al., 2016b, 2015a).

3. Material parameters identification

The anisotropy parameters should be determined such that the yield criterion reproduces the material's mechanical behavior as close as possible. The most commonly used experimental results for the identification of anisotropy parameters are the yield stresses and r-values obtained from in-plane tension for different angles (θ) with the rolling direction. When adopting classical methodologies, usually these tests are performed for several directions in the sheets plane (generally, 0°, 15°, 30°, 45°, 60°, 75° and 90° from the rolling direction). For some criteria, it is also recommended to know the experimental results for other trajectories, like the biaxial yield stress, σ_b, and the biaxial anisotropy coefficient r_b (Barlat et al., 2003; Lege et al., 1989; Pöhlandt et al., 2002). In case of yield criteria capable of describing SD effects, uniaxial compression experimental results are also necessary for describing the materials mechanical behavior for these stress states, ideally for the three axis of orthotropy. However, in order to characterize thin metallic sheets mechanical behavior for compression stress states, the use of small size specimens is necessary to avoid buckling effects. This leads to supplementary difficulties in the acquisition and analysis of the experimental results, particularly for high strain values (see e.g. Barlat et al., 1991b; Lege et al., 1989; Tritschler et al., 2014; Yoon et al., 2000).

The DD3MAT in-house code allows determining yield criterion parameters that accurately adjust a given material's experimental behavior (Barros et al., 2016c). Those parameters can then be used in the numerical simulation of forming processes, using the in-house code DD3IMP, where the yield are criteria implemented (Menezes and Teodosiu, 2000; Neto et al., 2015; Oliveira et al., 2008). The procedure adopted in DD3MAT is based on the minimization of an error function, which evaluates the difference between the estimated values and experimental ones, in the form

$$\begin{aligned} F(\mathbf{A}) = {} & w_{\sigma_\theta^T}\sum_{\theta=0}^{90}\left(\sigma_\theta^T(\mathbf{A})/\sigma_\theta^T - 1\right)^2 + w_{\sigma_\theta^C}\sum_{\theta=0}^{90}\left(\sigma_\theta^C(\mathbf{A})/\sigma_\theta^C - 1\right)^2 \\ & + w_{r_\theta}\sum_{\theta=0}^{90}\left(r_\theta(\mathbf{A})/r_\theta - 1\right)^2 + w_{\tau_\theta}\sum_{\theta=0}^{90}\left(\tau_\theta(\mathbf{A})/\tau_\theta - 1\right)^2 \\ & + w_{\sigma_b}(\sigma_b(\mathbf{A})/\sigma_b - 1)^2 + w_{r_b}(r_b(\mathbf{A})/r_b - 1)^2 \end{aligned} \tag{10}$$

where $\mathbf{A}$ represents the set of parameters associated with the selected yield criterion. σ_θ^T, σ_θ^C and r_θ are the experimental yield stresses in tension, compression and anisotropy coefficients determined in uniaxial tension, respectively, obtained from the uniaxial tests for a specific orientation (θ) with respect to the rolling direction. τ_θ is the experimental yield stress in shear, obtained for a specific orientation (θ) with respect to the rolling direction. σ_b is the experimental yield stress obtained from the equibiaxial tensile test and r_b is the experimental anisotropy coefficient obtained from the disc compression test. $\sigma_\theta^T(\mathbf{A})$, $\sigma_\theta^C(\mathbf{A})$ $r_\theta(\mathbf{A})$, $\tau_\theta(\mathbf{A})$, $\sigma_b(\mathbf{A})$ and $r_b(\mathbf{A})$ are the correspondent values predicted from the adopted yield criterion. Such procedure can be considered a generalization of the one proposed by Banabic et al. (2005), where the weighting factors, $w_{\sigma_\theta^T}$, $w_{\sigma_\theta^C}$, w_{r_θ}, w_{τ_θ}, w_{σ_b} and w_{r_b} are used to balance the influence of the experimental data. Nevertheless, the selection of the weighting factors is normally a manual procedure, strongly dependent on users' expertise and knowledge. In practice, this means that a first identification is always performed, considering unitary weights, to evaluate which experimental values are being reasonably well capture or not. Afterwards, the user can manually adjust each weighting factor, balancing the improvement in the fit of a specific experimental value, with the inevitable loss in the accuracy for the others. Since the identification procedure is sensitive to the weights considered for each experimental value, the adoption of this procedure introduces subjectivity in the definition of the best fit.

The experimental yield stress values can be used normalized with the yield stress given by the hardening law adopted. Nevertheless, the approach adopted in DD3MAT also allows considering that they correspond to the flow stress given by the hardening law for a certain equivalent plastic strain value, as long as the hardening law has been previously defined. This strategy enables the adoption of flow stress values determined for the same level of accumulated plastic work, in order to minimize inaccuracies related with the evaluation of the transition between the elastic and plastic behavior as well as some small changes in the yield surface shape (Barlat et al., 1997a).

The yield criteria parameters identification problem can be as simple as a resolution of a system of equations, when the number of experimental data is equal to the minimum necessary input data, or an optimization problem, when the number of experimental data is higher than the minimum necessary. The optimization algorithm adopted in DD3MAT is based on a downhill-simplex derivative free method, allowing to find the minimum of the objective function in a multidimensional space, with a low computational cost.

4. Cup drawing of a circular blank

The numerical simulation of the drawing of a circular cup is performed in order to analyze the influence of considering the SD effect in the final cup's geometry. This test is based on the work of Yoon et al. (2000) and was chosen since it involves tensile and compressive stress states. In fact, as long as the stress component

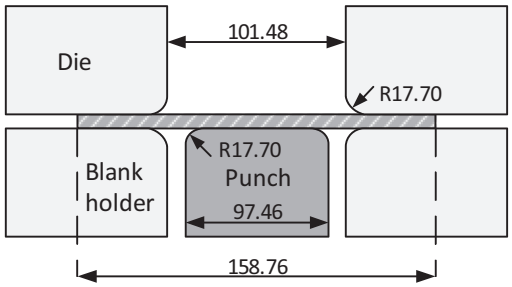

Fig. 1. Schematic of the cup drawing and main dimensions.

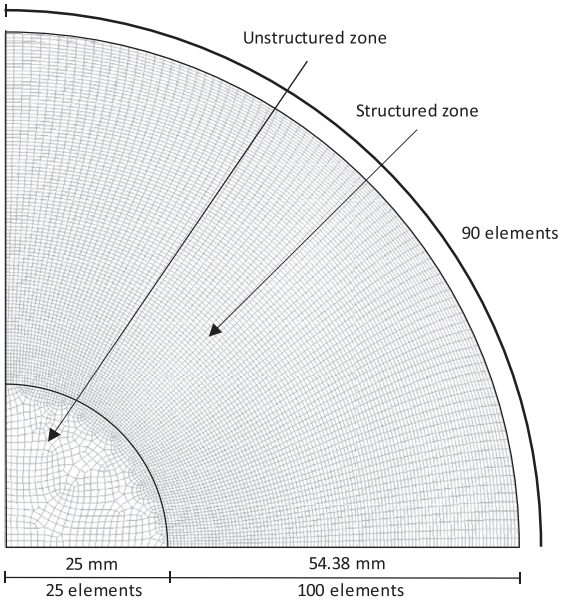

Fig. 2. In-plane blank sheet discretization.

in the thickness direction is small, the outer flange will be submitted to a compression stress state and the earing profile will be mainly dictated by the in-plane distribution of the yield stress and r-value (Yoon et al., 2011). For a material presenting SD effect, the in-plane distribution of the yield stresses in tension and compression can be quite different, meaning that it is expected to be able to evaluate the impact of taking into account the tension-compression asymmetry in the earing profile prediction.

4.1. Problem description

The schematic of the cup drawing process, together with the main dimensions, is shown in Fig. 1. Due to geometrical and material symmetries, only a quarter of the global structure is modeled. The contact with friction conditions is described by Coulomb's law, with a constant friction coefficient, μ, of 0.1. The blank sheet is circular in shape with a radius of 158.76 mm and thickness of 1.6 mm. The blank-holder force has a value of 22.2 kN, corresponding to the minimum value predicted to avoid wrinkling. Although not shown here, for this blank-holder force it is observed that the stress state component in the thickness direction is small, until a punch displacement of approximately 25 mm, thus not altering the compression stress state in the circumferential direction, for the material points located in the outer flange (Barros et al., 2016a).

The sheet is discretized with 8-node hexahedral finite elements, combined with a selective reduced integration technique (Hughes, 1980). Fig. 2 shows the in-plane sheet discretization used, highlighting the refined mesh adopted in the structured zone. Two elements are used in the thickness direction, leading to a total of 19,648 elements.

Table 1
Experimental uniaxial tension and compression yield stresses and r-values for the 2090-T3 aluminum alloy (Barlat et al., 1991b).

Test direction [°]	r-value	$\sigma_\theta^{Y_T}$ [MPa]	$\sigma_\theta^{Y_C}$ [MPa]	Stress ratio
0°	0.210	279.62	248.02	$\sigma_{RD}^{T}/\sigma_{RD}^{C}=1.127$
15°	0.330	269.72	260.75	
30°	0.690	255.00	255.00	
45°	1.580	226.77	237.75	
60°	1.050	227.50	245.75	
75°	0.550	247.20	263.75	
90°	0.690	254.45	266.48	$\sigma_{TD}^{T}/\sigma_{TD}^{C}=0.955$
σ_b		289.40		
r_b	0.670			

4.2. Material mechanical behavior

The yield criteria parameters are identified considering the experimental data for the 2090-T3 aluminum alloy presented in Table 1, which considers experimental uniaxial tension and compression yield stresses, as well as the anisotropy coefficients for different orientations with the rolling direction. The experimental yield stress and r-value obtained from the balance biaxial test and disk compression test are also presented (Barlat et al., 1991b).

This work considers a fixed value of $a=2$ for the CPB06 yield criterion. Assuming this condition, three different sets of anisotropy parameters were identified, considering: (i) $k \neq 0$ and all the experimental data available, allowing for the modeling of tension-compression asymmetry (labeled "CPB06"); (ii) $k=0$ and neglecting the experimental compression yield stresses (labeled "CPB06 $k=0$ T"); and (iii) $k=0$ and neglecting the experimental tensile yield stresses (labeled "CPB06 $k=0$ C"). For the particular case of the CPB06 with one linear transformation, adopted in this work, the yield criterion presents 9 anisotropy parameters and the k value. When considering thin metallic sheets, the off-plane properties are difficult to obtain. Thus, the corresponding anisotropy parameters, C_{44} and C_{55}, cannot be evaluated and, therefore, the corresponding isotropic values are commonly adopted, i.e. 1.0. Moreover, the C_{11} parameter is also considered equal to 1.0 due to the homogeneity of the criterion. The adoption of this condition eliminates the possibility of obtaining non-unique sets of parameters, i.e. sets with symmetrical values for k and the C_{ij} parameters that lead to the same value for the objective function, as previously reported in (Barros et al., 2016b). In brief, it is necessary to identify a total of 6 anisotropy parameters and the k value. The identification procedure assumes that $k \in [-1, 1]$ and $C_{ij} \in [-4, 6]$.

For the CB2001 yield criterion, only one set of anisotropy parameters was identified, considering all the experimental data available, except the compression yield stresses (labeled "CB2001"). For this yield criterion, the parameters a_5,a_6 and b_k ($k=6, 7, 8, 9, 11$) correspond to the off-plane properties, which cannot be evaluated and, consequently, are assumed as equal to the isotropic values, i.e. 1.0. It is also assumed that $a_i \in [-10, 10]$, $b_i \in [-10, 10]$ and $c \in [-3.75, 2.25]$. The minimization process adopted for this yield criterion includes testing the convexity of the yield surface, for several planes in the stress space (Barros et al., 2015a).

For both yield criteria the minimization problem associated to Eq. (10) is over constrained, since a total of 23 experimental values are used to identify only 7 parameters in case of CPB06, and 11 parameters in case of CB2001. In case of CPB06, when neglecting the SD effect, a total of 16 experimental values were considered.

The plastic behavior is described using an isotropic work hardening Swift type law, given by

$$Y(\bar{\varepsilon}^p) = K(\varepsilon_0 + \bar{\varepsilon}^p)^n, \tag{11}$$

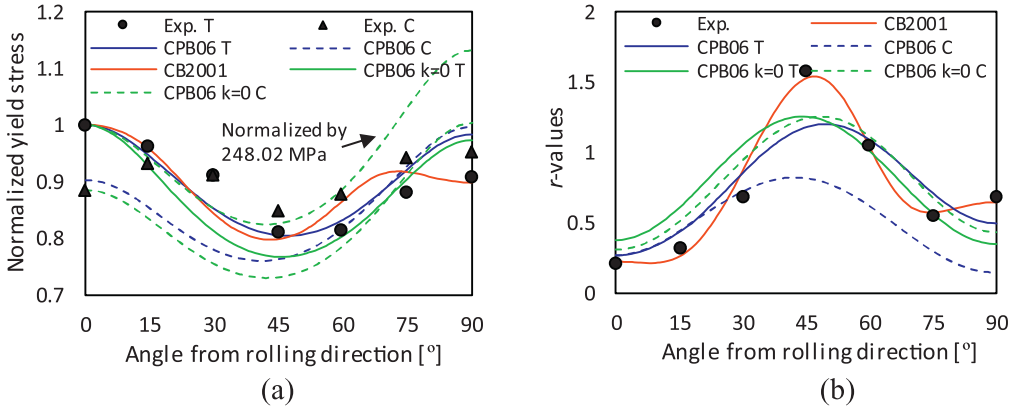

Fig. 3. Experimental and predicted in-plane evolution of the: (a) yield stress (normalized with Y_0) and (b) r-value, for the 2090-T3 aluminum alloy. (For interpretation of the references to color in this figure legend, the reader is referred to the web version of this article.)

Table 2
Elastic properties and material parameters of the work hardening law Yoon et al., (2000).

Elastic properties	Isotropic hardening (Swift law)	
	CPB06 $k=0$ C	All other cases
$E=74$ [GPa]	$K=670$ [MPa]	$K=646$ [MPa]
$\upsilon=0.34$	$\varepsilon_0=0.0183$	$\varepsilon_0=0.0250$
	$n=0.2485$	$n=0.2270$
	$Y_0=248.02$ [MPa]	$Y_0=279.62$ [MPa]

where Y is the flow stress and $\bar{\varepsilon}^p$ is the equivalent plastic strain. The material's mechanical behavior is assumed to be isotropic in the elastic regime, being described by the Young's modulus, E, and the Poisson ratio, υ.

Note that the CPB06 criterion guarantees that the yield stress Y_0 considered is always equal to the one obtained for the uniaxial tensile test performed along the rolling direction, σ^T_{RD}. Previous results indicate that the value proposed for the yield stress, Y_0, defined by the hardening law, should be in accordance with σ^T_{RD}, to enable an accurate description of the in-plane yield stress directionalities (Barros et al., 2015b). Following this recommendation, the parameters adopted for the Swift hardening law consider a yield stress value $Y_0=279.62$ MPa, for anisotropy coefficients identified considering the tensile yield stress in-plane distribution. For the same reason, for the case "CPB06 $k=0$ C" it is necessary to assume $Y_0=248.02$ MPa. Therefore, a new set of parameters for the hardening law were determined by minimizing the difference in the plastic work attained by the two hardening laws, for an equivalent plastic strain value of 0.5. A summary of the elastic properties and the hardening law parameters is presented in Table 2.

The considered weighting coefficients for each criterion are presented in Table 3, while the identified anisotropy parameters are the ones presented in Table 4. Fig. 3 presents the experimental and numerically predicted yield stresses and anisotropy coefficients for the four cases. The "CPB06" identification is able of simultaneously predict the evolution of the yield stresses in tension and in compression. The evolution of the tension yield stress is globally well predicted, with the minimum occurring for 45° while from this angle forward the values are over predicted. As for the evolution of the compression yield stresses, the main shape of the evolution is captured. For this identification, since $k\neq 0$, the r-values evolution is also different for tension and compression. The tensile r-values show the same trend as the experimental ones with the lowest value at 0° and maximum at about 45°. Regarding the compression r-values no analysis can be performed, since the experimental values are not known. Nonetheless, the results are shown to highlight the difference in the predicted values. The stress ratios predicted are $\sigma^T_{RD}/\sigma^C_{RD}=1.106$ and $\sigma^T_{TD}/\sigma^C_{TD}=0.985$, which means that they are, respectively, slightly under and overestimated, with a relative difference inferior to 5% (see Table 1). Finally, it should be mentioned that since one linear transformation was adopted, the yield criterion is not flexible enough to describe the highly orthotropic in-plane behavior of this aluminum alloy.

The CB2001 allows an excellent description of both tensile yield stresses and r-values directionalities but, since it is unable to describe the SD effect, the stress ratio in the three principal axis is always equal to 1.0. The same stress ratios are valid for the identifications performed with $k=0$. Regarding the "CPB06 $k=0$ T" identification, the evolution of the tensile yield stresses and r-values is relatively well captured. For the "CPB06 $k=0$ C" identification, since the input yield stresses were the compression ones, in Fig. 3(a) a second green dashed curve is used to present a normalization with the yield stress value $Y_0=279.62$ MPa, enabling its comparison with the experimental ones. This way it is possible to confirm that the evolution is globally well predicted. The predicted r-values are very close to the previous case, "CPB06 $k=0$ T", enabling the analysis of the influence of the compression yield stress directionalities.

The values predicted for the biaxial yield stress and biaxial anisotropy coefficient are presented in Table 5. These results are highlighted in Fig. 4, which presents the corresponding yield surfaces in both the σ_1,σ_2 plane ($\sigma_3,\sigma_{12}=0$) and the π-plane. All three CPB06 cases fail to recover the biaxial yield stress value, underestimating it. The CB2001, however, presents a good fit. As for the biaxial anisotropy coefficient, all the CPB06 cases overestimate this value, with the "CPB06 $k=0$ T" presenting the worst prediction. The CB2001 presents a very accurate fit for this value.

4.3. Results and discussion

The numerically predicted punch force and blank-holder displacement with the punch displacement are presented in Fig. 5. Even though no experimental results are available for comparison purposes, these results are shown to highlight the importance of the material mechanical behavior in the process conditions. Regarding the four cases, the results show that the punch force increases until attaining a maximum value for a punch displacement of about 31 mm, corresponding approximately to the instant where the blank-holder displacement is maximum. From this instant, the punch force decreases and, in some cases, presents a stepped decrease when the blank-holder loses contact with the blank, as seen from the dashed curves corresponding to the blank-holder displacement. Afterwards, an increase in the punch force is observed,

Table 3
Weighting coefficients used in the identification procedure (if not presented, assume as 1.0).

CB2001	$w_{r_{45}} = 5\ w_{r_{75}} = 5\ w_{r_{90}} = 5\ w_{\sigma_b} = 20\ w_{\sigma^T_{60}} = 10\ w_{\sigma^T_{75}} = 10\ w_{\sigma^T_{90}} = 10$
CPB06	$w_{r_{45}} = 7\ w_{\sigma_b} = 20\ w_{\sigma^T_{90}} = 30\ w_{\sigma^C_{15}} = 40\ w_{\sigma^C_{30}} = 5\ w_{\sigma^C_{45}} = 5\ w_{\sigma^C_{60}} = 5\ w_{\sigma^C_{75}} = 5\ w_{\sigma^C_{90}} = 40$
CPB06 $k=0$ T	$w_{r_0} = w_{r_{15}} = w_{r_{30}} = w_{r_{60}} = w_{r_{75}} = w_{r_{90}} = 0.1w_{\sigma_b} = 10w_{\sigma^T_{60}} = 10w_{\sigma^T_{75}} = 20w_{\sigma^T_{90}} = 50$
CPB06 $k=0$ C	$w_{r_0} = 0.7w_{r_{15}} = 0.2w_{r_{30}} = w_{r_{60}} = 0.5w_{r_{45}} = 5w_{\sigma_b} = 10w_{\sigma^T_{60}} = 10w_{\sigma^T_{75}} = 20w_{\sigma^T_{90}} = 50$

Table 4
Identified parameters for the 2090-T3 aluminum alloy for the considered yield criteria.

CB2001	a_1		a_2		a_3		a_4	
	1.358		1.848		1.075		1.709	
	b_1	b_2	b_3	b_4		b_5	b_{10}	c
	5.357	−0.623	−4.386	−3.654		−6.046	−0.882	0.857
	C_{11}	C_{22}	C_{33}	C_{66}	C_{23}	C_{13}	C_{12}	k
CPB06	1.000	−0.473	−1.381	1.421	0.151	0.119	0.999	0.050
CPB06 $k=0$ T	1.000	0.987	1.019	1.134	0.006	0.036	0.195	0.000
CPB06 $k=0$ C	1.000	1.013	1.007	−1.162	0.057	−0.059	0.196	0.000

Table 5
Experimental and numerically predicted biaxial yield stress and anisotropy coefficient for the 2090-T3 aluminum alloy.

	Experimental	CB2001	CPB06	CPB06 $k=0$ T	CPB06 $k=0$ C
σ_b [MPa]	287.48	285.89	229.48	228.13	216.63
r_b	0.67	0.660	0.893	1.078	0.710

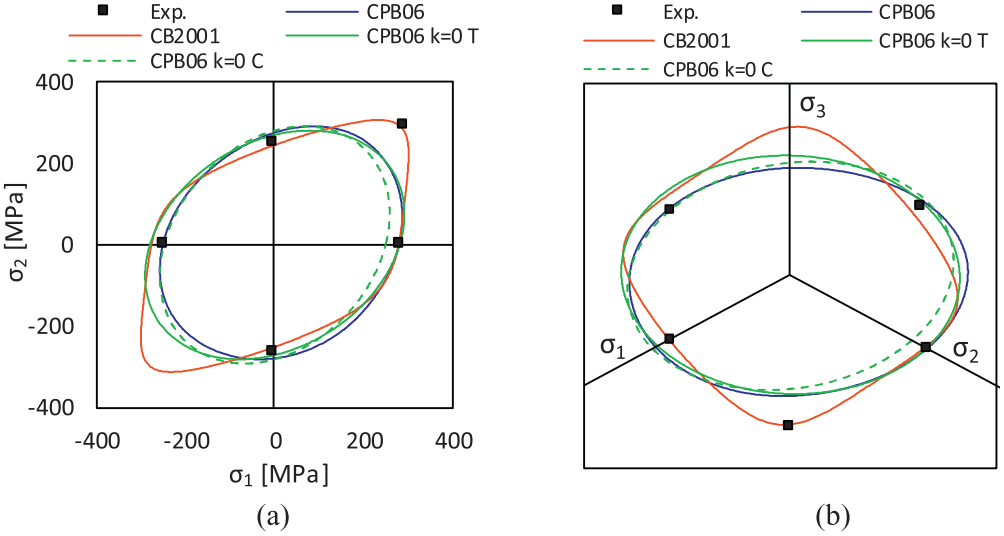

Fig. 4. Predicted yield surfaces in the (a) σ_{11},σ_{22} plane (with $\sigma_{33}=0$) and (b) π-plane (normalized with the yield stress value of $Y_0=279.62$ MPa).

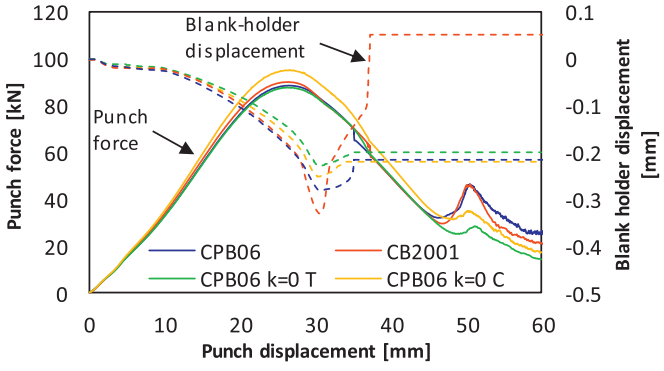

Fig. 5. Numerically predicted punch force and blank-holder displacement evolutions with punch displacement. Solid lines represent the punch force and dashed lines represent the blank-holder displacement.

between 47 mm and 52 mm of punch displacement, corresponding to the ironing of the cup's flange between the punch and the die. The lower punch force values for the ironing stage, occur for both cases of the CPB06 with $k=0$, since they present a lower value for the flange thickening, as shown in Fig. 6. Fig. 6 also shows that the "CPB06 $k=0$ T" presents a thickness strain distribution in the flange which is more uniform than the other cases. Since both CPB06 cases with $k=0$ describe the in-plane r-values similarly, the observed differences can be related with the in-plane yield stress distribution. For the "CPB06 $k=0$ T", the thickness strain distribution in the flange is more uniform than in the "CPB06 $k=0$ C" because, although the in-plane yield stress distribution presents a similar trend, the amplitude of variation is smaller for the "CPB06 $k=0$ T" (see Fig. 3(a)). The "CPB06 $k=0$ C" presents a higher thickening of the flange mainly for angles closer to the transverse direction, as shown in Fig. 6(d), which is a direct result of the fact that the yield stresses are higher for angles closer to this direction. In

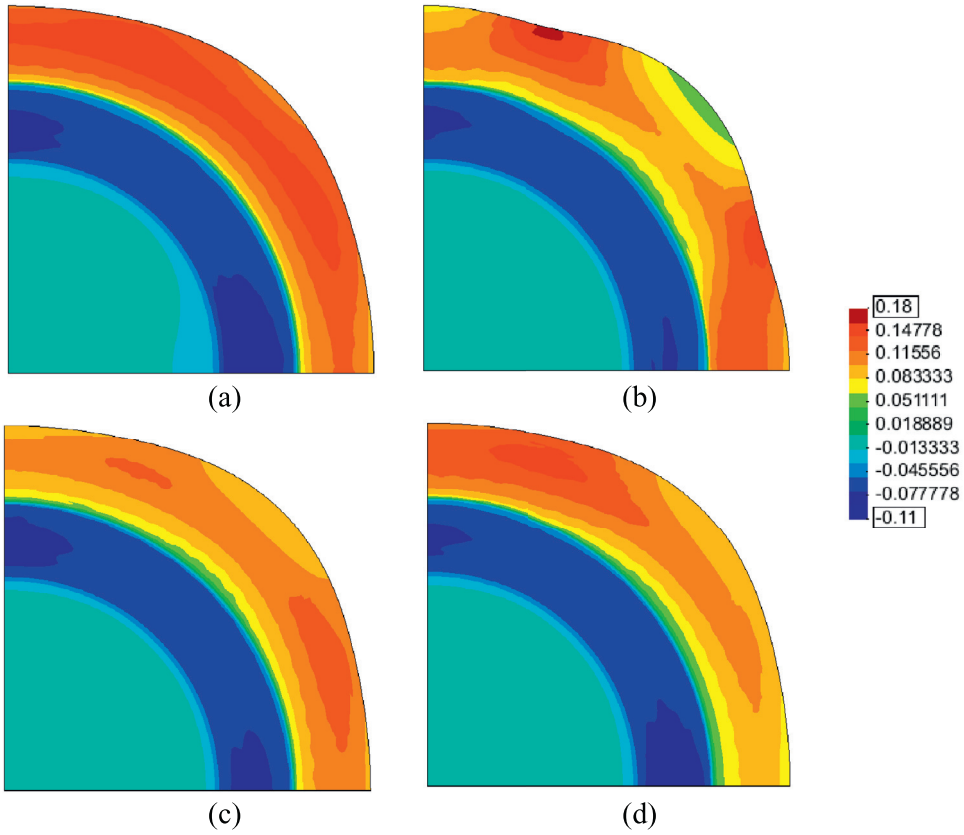

Fig. 6. Through-thickness strain distribution, for a punch displacement of 30 mm for the: (a) CPB06; (b) CB2001; (c) CPB06 $k=0$ T and (d) CPB06 $k=0$ C.

fact, the ratio between the yield stresses in RD and TD, $\sigma_{RD}^{T}/\sigma_{TD}^{T}$ are 1.028 and 0.882 for the "CPB06 $k=0$ T" and the "CPB06 $k=0$ C", respectively.

The analysis of the influence of the predicted yield stresses and anisotropy coefficients evolution in the predicted cup height, must take into account the ones corresponding to compression, since the in-plane compression stress state is the one predominant in the flange area (Yoon et al., 2011). Also, other authors have shown, considering the present example of the drawing of a circular cup, that both the compression yield stresses and the anisotropy coefficients in the rolling direction will have a direct impact on the material behavior at the transverse direction and *vice-versa*. In fact, the behavior of the rim in the direction defined by θ with the rolling direction is controlled by the material compression properties in the direction defined by $90-\theta$ (Chung et al., 2011; Mulder and Vegter, 2011; Yoon et al., 2011). Based on these results, Yoon et al. (2011) proposed an analytical function to estimate the cup height directionality,

$$H^{\text{cup}}(\theta) = t_0 + r_c + \frac{R_b}{A_{\theta+90}+1}\left(d^{A_{\theta+90}} - \frac{1}{d}\right)B_\theta{}^{A_{\theta+90}}, \tag{12}$$

where t_0 is the initial blank thickness, R_b is the blank radius and r_c is the radius of the cup defined by the punch fillet radius. The r-value and the yield stress directionalities influence is dictated by

$$A_{\theta+90} = \frac{r_{\theta+90}}{1+r_{\theta+90}} \text{ and } B_\theta = \left(\frac{\sigma_{\text{ref}}}{\sigma_\theta^{T}}\right)^{\beta'} \tag{13}$$

respectively. Assuming that the uniaxial tension and compression lead to identical r-values, these can be expressed as a function of the plastic strains at the rim

$$r_{\theta+90} = \frac{\varepsilon_r}{\varepsilon_t} = -\frac{\varepsilon_r}{\varepsilon_r+\varepsilon_\theta}, \tag{14}$$

were subscripts r, θ and t correspond to the radial, circumferential and thickness directions, respectively. It is also assumed that the radial tension can be modelled from the yield stress directionality σ_θ^{T}, such that

$$\sigma^{\text{ref}} = \frac{\int_0^{2\pi}\sigma_\theta^{T}\mathrm{d}\theta}{2\pi} = \frac{1}{12}\left[\sigma_0^{T}+2\left(\sigma_{15}^{T}+\sigma_{30}^{T}+\sigma_{45}^{T}+\sigma_{60}^{T}+\sigma_{75}^{T}\right)+\sigma_{90}^{T}\right], \tag{15}$$

for an orthotropic material, for which data is known for every 15°. The deceleration β' factor is introduced to take into account the variation of the stress mode along the flange, i.e. $\beta'=1$ corresponds to the assumption that the stress mode at the inner most flange is applied to the entire flange; $\beta'=0.5$ corresponds to a linear distribution of the radial tensile stress; the recommended value is $0.5 \le \beta' \le 1$. Finally, d corresponds to the ratio between the blank radius R_b and the cup radius R_c.

This analytical function shows that a lower value of the anisotropy coefficient leads to lower cup height whereas lower values of the yield stresses lead to a higher cup height (Yoon et al., 2011). The cup height was estimated for all cases under analysis using Eq. (12), considering $\beta'=0.5$ and the predicted in-plane yield stress and r-value distribution. Note that, for the "CPB06" two cases where considered: (i) using the tensile yield stress and r-values (labeled "CPB06 T") and (ii) using the compression yield stresses and r-values (labelled "CPB06 C"). The results obtained for the cup height, normalized by the experimental cup height at RD, are shown in Fig. 7(a). For this particular case, the earing profile is mainly dictated by the r-value in-plane distribution, which is supported by the comparison of its trend with the one shown in Fig. 3(b). Moreover, it is possible to confirm that for the "CPB06 $k=0$ C" the cup height attains the higher values, while the "CPB06 C" leads to the lowest ones, has a consequence of the similar yield

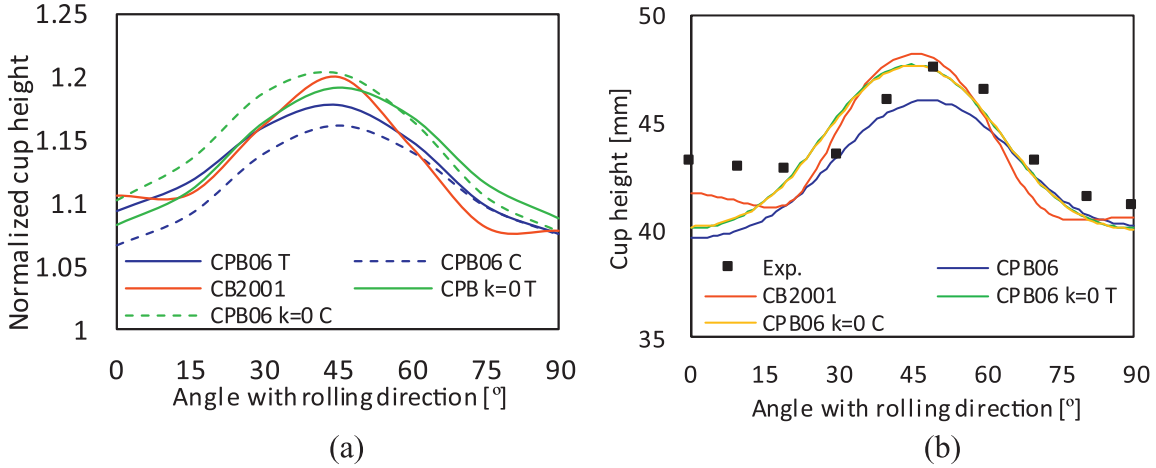

Fig. 7. (a) Analytically predicted normalized cup height; and (b) experimental and numerically predicted cup height, vs. angle from rolling direction.

stress distribution and the lower compression *r*-values. The comparison of the results obtained with both CPB06 cases with $k=0$, which present a similar in-plane distribution for the *r*-values, confirms that the yield stress in-plane distribution presents a small effect, which can be related with its small amplitude of variation.

Fig. 7(b) presents the comparison between experimental and numerically predicted cup height vs. angle from rolling direction, after the drawing operation. Regarding the earing profile, globally the shape is well predicted by for cases, with the maximum height at about 45°. Also, the average height is within the experimental values. However, the increased experimental height at 0° is not predicted by any of the CPB06 identifications, which can be attributed to the fact that this yield criterion, considering only one linear transformation, is not flexible enough to predict more than 4 ears. In fact, the CB2001 can predict the higher height for 0° as a direct consequence of the good prediction of both yield stresses and *r*-values directionalities (Fig. 3). The differences in height between the "CPB06" and both cases of the CPB06 with $k=0$ can be attributed to the difference in the predicted *r*-values for the compression state, with both "CPB06 $k=0$ T" and "CPB06 $k=0$ C" predicting similar values, which are higher than the ones predicted by the "CPB06" for approximately 30° and forward. The differences between "CPB06 $k=0$ T" and "CPB06 $k=0$ C" are negligible. These results follow the trend observed in the analytical prediction (see Fig. 7(b)), although numerically the effect of the in-plane yield stress distribution becomes even more irrelevant. In this context it should be mentioned that, although not shown here, for a punch displacement of approximately 25 mm, the contact conditions change in the flange area and the stress state component in the thickness direction alters the compression stress state in the circumferential direction, for the material points located in the outer flange (Barros et al., 2016a). This stress state change is slightly more evident for the "CPB06 $k=0$ C" than for the "CPB06" and the "CPB06 $k=0$ T", due to the higher difference in the thickness distribution in the flange area (see Fig. 6(d)). The contact conditions in the flange area influence the earing profile predicted, particularly for materials with a strong anisotropic behavior of the *r*-values (Barros et al., 2015a). This influence of the contact conditions also justifies the differences between the predictions obtained with the analytical function and the numerical simulation. For this particular case, the analytical function overestimates the cup height, but enables an analysis of the effect of the yield stress and *r*-value in-plane distribution in the earing profile.

Fig. 8 presents the thickness strains evolution along the cup, measured experimentally and the ones predicted numerically. Globally, the thickness strain is well predicted in all cases, with a reduction for an initial material position of about 40 mm, corresponding to the punch radius. From about 60 mm forward, a thickening is observed both experimentally and numerically. Globally the thickening is overestimated, whichever case considered, which can be related to the lower average height estimated for the cup (see Fig. 7(b)). Regarding the experimental trend, the thickness strain in the rolling direction is lower than the one in the transverse direction. The "CPB06" globally captures this trend, while the "CB2001" presents the opposite behavior (see Fig. 8(a)). The "CPB06 $k=0$ T" presents the same behavior as the "CB2001", while "CPB06 $k=0$ C" is able to describe the differences between the rolling and the transverse direction (see Fig. 8(b)). In fact, the "CPB06 $k=0$ C" presents a higher difference between the RD and the TD thickness strains than the "CPB06" case. This can be related with the ratio between the compression yield stress in RD and TD, $\sigma^{C}_{RD}/\sigma^{C}_{TD}$, with an experimental value of 0.931. The "CPB06 $k=0$ C" and the "CPB06" present values of 0.882 and 0.905, respectively. Thus, a higher value for the compression yield stress along TD, when compared with the one for RD (see Fig. 3), leads to a higher thickening in the transverse direction, as shown in Fig. 6. This also explains why the "CB2001" and the "CPB06 $k=0$ T" cannot capture this effect, since they impose the same trend for the tensile and compressive yield stress, with the $\sigma^{C}_{RD}/\sigma^{C}_{TD}$ ratios equal to 1.113 and 1.028, respectively. Thus, the yield stress at RD is higher than for TD. These results indicate that it is important to capture the ratio $\sigma^{C}_{RD}/\sigma^{C}_{TD}$ in order to improve the thickness prediction. Moreover, it is known that the *r*-value dictates the thickness strain, which as previously mentioned, should be the one for the compression state, but its experimental values unfortunately are unavailable.

5. Conclusions

The numerical simulation of the drawing of a cylindrical cup was performed considering a 2090-T3 aluminum alloy, with two yield criteria. The results highlight the importance of an accurate description of the material yield stresses and *r*-values in-plane directionalities, for compression stress states, in order to have more accurate predictions of both the earing profile and the thickness distributions. In fact, for the example under analysis, the results show that the earing profile is mainly dictated by the compression *r*-values in-plane directionalities, which are commonly unavailable for thin metallic sheets. The adoption of a yield criterion that takes into account the SD effect, combined with an associated flow rule, enables the simultaneous prediction of both compression yield stress and *r*-values directionalities. The compression yield

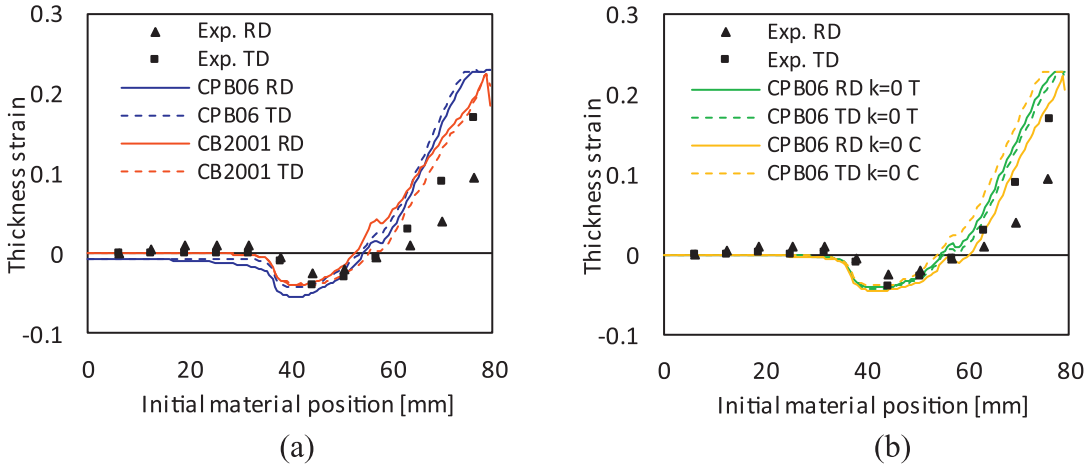

Fig. 8. Experimental and numerically predicted thickness strain for the rolling and transverse directions for the (a) CPB06 and CB2001 and (b) CPB06 $k=0$ T and CPB06 $k=0$ C. Solid lines used for the RD while dashed lines are used for the TD.

stresses directionalities seem to play a major role in the thickness prediction. The adoption of a flexible yield criterion, such as the CB2001, allows a proper prediction of the earing profile, but fails to capture the trend for the thickness distribution, since it imposes the same trend for the tensile and compression yield stresses directionalities. Following these conclusions, it is recommended the use of a yield criterion that is flexible enough to describe both the yield stresses and *r*-values directionalities, including the ones in compression, even for materials presenting a small SD effect. In this context, the use of the CPB06 with two linear transformations will be analyzed in a future work.

Acknowledgment

The authors gratefully acknowledge the financial support of the Portuguese Foundation for Science and Technology (FCT) under projects with reference PTDC/EMS-TEC/0702/2014 (POCI-01- 0145-FEDER-016779) and PTDC/EMS-TEC/6400/2014 (POCI-01-0145-FEDER-016876) by UE/FEDER through the program COMPETE 2020. The first author is also grateful to the FCT for the PhD grant SFRH/BD/98545/2013.

References

Banabic, D., 2010. Sheet Metal Forming Processes. Springer. Springer-Verlag, Berlin Heidelberg doi:10.1007/978-3-540-88113-1.

Banabic, D., Aretz, H., Comsa, D.S., Paraianu, L., 2005. An improved analytical description of orthotropy in metallic sheets. Int. J. Plast. 21, 493–512. doi:10.1016/j.ijplas.2004.04.003.

Banabic, D., Balan, T., Comsa, D.S., 2000. A new yield criterion for orthotropic sheet metals under plane stress conditions. In: 7th Cold Met. Form. Conf., pp. 217–224. doi:10.1016/S0020-7403(03)00139-5.

Barlat, F., Aretz, H., Yoon, J.W., Karabin, M.E., Brem, J.C., Dick, R.E., 2005. Linear transfomation-based anisotropic yield functions. Int. J. Plast. 21, 1009–1039. doi:10.1016/j.ijplas.2004.06.004.

Barlat, F., Becker, R.C., Hayashida, Y., Maeda, Y., Yanagawa, M., Chung, K., Brem, J.C., Lege, D.J., Matsui, K., Murtha, S.J., Hattori, S., 1997a. Yielding description for solution strengthened aluminum alloys. Int. J. Plast. 13, 385–401. http://dx.doi.org/10.1016/S0749-6419(97)80005-8.

Barlat, F., Brem, J.C., Yoon, J.W., Chung, K., Dick, R.E., Lege, D.J., Pourboghrat, F., Choi, S.H., Chu, E., 2003. Plane stress yield function for aluminum alloy sheets - part 1: theory. Int. J. Plast. 19, 1297–1319. doi:10.1016/S0749-6419(02)00019-0.

Barlat, F., Lege, D.J., Brem, J.C., 1991a. A six-component yield function for anisotropic materials. Int. J. Plast. 7, 693–712. doi:10.1016/0749-6419(91)90052-Z.

Barlat, F., Lege, D.J., Brem, J.C., Warren, C.J., 1991b. Constitutive behavior for anisotropic materials and application to a 2090 Al±Li alloy. In: Lowe, T., Rollett, A., Follansbee, P., Daehn, G. (Eds.), TMS Annual Meeting. TMS, New Orleans, LA, pp. 189–203.

Barlat, F., Maeda, Y., Chung, K., Yanagawa, M., Brem, J.C., Hayashida, Y., Lege, D.J., Matsui, K., Murtha, S.J., Hattori, S., Becker, R.C., Makosey, S., 1997b. Yield function development for aluminum alloy sheets. J. Mech. Phys. Solids 45, 1727–1763. doi:10.1016/S0022-5096(97)00034-3.

Barros, P.D., Alves, J.L., Oliveira, M., Menezes, L.F., 2016a. Tension-compression asymmetry modelling: strategies for anisotropy parameters identification. NUMIFORM 2016: The 12th International Conference on Numerical Methods in Industrial Forming Processes. MATEC Web of Conferences doi:10.1051/matecconf/20168005002.

Barros, P.D., Alves, J.L., Oliveira, M.C., Menezes, L.F., 2016b. Modeling of tension-compression asymmetry and orthotropy on metallic materials: numerical implementation and validation. Int. J. Mech. Sci. 114, 217–232. doi:10.1016/j.ijmecsci.2016.05.020.

Barros, P.D., Carvalho, P.D., Alves, J.L., Oliveira, M.C., Menezes, L.F., 2016c. DD3MAT - a code for yield criteria anisotropy parameters identification. J. Phys. doi:10.1088/1742-6596/734/3/032053.

Barros, P.D., Neto, D.M., Alves, J.L., Oliveira, M., Menezes, L.F., 2015a. DD3IMP, 3D fully implicit finite element solver: implementation of CB2001 yield criterion. Rom. J. Tech. Sci. Appl. Mech. 60, 105–136.

Barros, P.D., Oliveira, M.C., Alves, J.L., Andrade-Campos, A., Menezes, L.F., 2015b. Modelling of tension-compression asymmetry and orthotropic anisotropy in case of thin metallic sheets: identification procedure and case studies. In: Hora, P. (Ed.), Institute of Virtual Manufacturing. ETH Zurich, Zurich, pp. 149–154.

Cazacu, O., Barlat, F., 2004. A criterion for description of anisotropy and yield differential effects in pressure-insensitive metals. Int. J. Plast. 20, 2027–2045. doi:10.1016/j.ijplas.2003.11.021.

Cazacu, O., Barlat, F., 2003. Application of the theory of representation to describe yielding of anisotropic aluminum alloys. Int. J. Eng. Sci. 41, 1367–1385. doi:10.1016/S0020-7225(03)00037-5.

Cazacu, O., Barlat, F., 2001. Generalization of Drucker's yield criterion to orthotropy. Math. Mech. Solids 6, 613–630. doi:10.1177/108128650100600603.

Cazacu, O., Plunkett, B., Barlat, F., 2006. Orthotropic yield criterion for hexagonal closed packed metals. Int. J. Plast. 22, 1171–1194. doi:10.1016/j.ijplas.2005.06.001.

Chung, K., Kim, D., Park, T., 2011. Analytical derivation of earing in circular cup drawing based on simple tension properties. Eur. J. Mech. A Solids 30, 275–280. doi:10.1016/j.euromechsol.2011.01.006.

Comsa, D.S., Banabic, D., 2007. Numerical simulation of sheet metal forming processes using a new yield criterion. Key Eng. Mater. 344, 833–840. doi:10.4028/www.scientific.net/KEM.344.833.

Drucker, D.C., 1949. Relation of experiments to mathematical theories of plasticity. J. Appl. Mech. ASME 16, A349–A357.

Hill, R., 1948. A theory of the yielding and plastic flow of anisotropic metals. Proc. R. Soc. A Math. Phys. Eng. Sci. 193, 281–297. doi:10.1098/rspa.1948.0045.

Hughes, T.J.R., 1980. Generalization of selective integration procedures to anisotropic and nonlinear media. Int. J. Numer. Methods Eng. 15, 1413–1418. doi:10.1002/nme.1620150914.

Lege, D.J., Barlat, F., Brem, J.C., 1989. Characterization and modeling of the mechanical behavior and formability of a 2008-T4 sheet sample. Int. J. Mech. Sci. 31, 549–563.

Menezes, L.F., Teodosiu, C., 2000. Three-dimensional numerical simulation of the deep-drawing process using solid finite elements. J. Mater. Process. Technol. 97, 100–106. doi:10.1016/S0924-0136(99)00345-3.

Mulder, J., Vegter, H., 2011. An analytical approach for earing in cylindrical deep drawing based on uniaxial tensile test results 1447, 1447–1452. doi:10.1063/1.3589720.

Neto, D.M., Oliveira, M.C., Menezes, L.F., 2015. Surface smoothing procedures in computational contact mechanics. Arch. Comput. Methods Eng. doi:10.1007/s11831-015-9159-7.

Oliveira, M.C., Alves, J.L., Menezes, L.F., 2008. Algorithms and strategies for treatment of large deformation frictional contact in the numerical simulation of deep drawing process. Arch. Comput. Methods Eng. 15, 113–162.

Plunkett, B., Lebensohn, R.a., Cazacu, O., Barlat, F., 2006. Anisotropic yield function of hexagonal materials taking into account texture development and anisotropic hardening. Acta Mater. 54, 4159–4169. doi:10.1016/j.actamat.2006.05.009.

Pöhlandt, K., Banabic, D., Lange, K., 2002. Equi-biaxial anisotropy coefficient used to describe the plastic behavior of sheet metal. In: ESAFORM 2002. Krakow, Poland, pp. 723–727.

Tresca, H.-É., 1864. Mémoire sur l'écoulement des corps solides soumis à de fortes pressions. Comptes Rendus l'Académie des Sci. Paris 59, 754–758.

Tritschler, M., Butz, A., Helm, D., Falkinger, G., Kiese, J., 2014. Experimental analysis and modeling of the anisotropic response of titanium alloy Ti-X for quasi-static loading at room temperature. Int. J. Mater. Form. 7, 259–273. doi:10.1007/s12289-013-1125-z.

von Mises, R., 1913. Mechanik der festen korper im plastic-deformablen zustand. Nachrichten vos der K. gellesschaft des winssenschaften zu Gottingen 582–592.

Yoon, J.W., Barlat, F., Chung, K., Pourboghrat, F., Yang, D.Y., 2000. Earing predictions based on asymmetric nonquadratic yield function. Int. J. Plast. 16, 1075–1104. doi:10.1016/S0749-6419(99)00086-8.

Yoon, J.W., Dick, R.E., Barlat, F., 2011. A new analytical theory for earing generated from anisotropic plasticity. Int. J. Plast. 27, 1165–1184. doi:10.1016/j.ijplas.2011.01.002.

Yoshida, F., Hamasaki, H., Uemori, T., 2013. A user-friendly 3D yield function to describe anisotropy of steel sheets. Int. J. Plast. 45, 119–139. doi:10.1016/j.ijplas.2013.01.010.